



1 **Aerosol Surface Area Concentration: a Governing Factor for New** 2 **Particle Formation in Beijing**

3 Runlong Cai^{1,#}, Dongsen Yang^{2,#}, Yueyun Fu¹, Xing Wang², Xiaoxiao Li¹, Yan Ma², Jiming Hao¹,
4 Jun Zheng^{2*} and Jingkun Jiang^{1*}

5 ¹State Key Joint Laboratory of Environment Simulation and Pollution Control, School of Environment, Tsinghua
6 University, Beijing, 100084, China

7 ²Collaborative Innovation Center of Atmospheric Environment and Equipment Technology, Nanjing
8 University of Information Science & Technology, Nanjing 210044, China

9 #: Runlong Cai and Dongsen Yang contribute equally to this work

10 *: Correspondence to: J. Jiang (jiangjk@tsinghua.edu.cn) and J. Zheng (zheng.jun@nuist.edu.cn)

11 **Abstract.** The predominating role of aerosol Fuchs surface area, A_{Fuchs} , in determining the occurrence of new particle
12 formation (NPF) events in Beijing was elucidated in this study. Analysis was based on a field campaign from March 12th
13 to April 6th, 2016, in Beijing, during which aerosol size distributions down to ~1 nm and sulfuric acid concentration were
14 simultaneously monitored. The 26 days were classified into 11 typical NPF days, 2 undefined days, and 13 non-event
15 days. A dimensionless factor, L_{Γ} , characterizing the relative ratio of the coagulation scavenging rate over the
16 condensational growth rate and predicting whether or not a NPF event would occur (Kuang et al., 2010), was applied.
17 The three parameters determining L_{Γ} are sulfuric acid concentration, the growth enhancement factor characterizing
18 contribution of other gaseous precursors to particle growth, Γ , and A_{Fuchs} . Different from other atmospheric environment
19 such as in Boulder and Hyytiälä, the variations of daily maximum sulfuric acid concentration and Γ in Beijing are in a
20 narrow range with geometric standard deviations of 1.40 and 1.31, respectively. Positive correlation was found between
21 estimated new particle formation rate, $J_{1.5}$, and sulfuric acid concentration with a mean fitted exponent of 2.4. However,
22 sulfuric acid concentration on NPF days is not significantly higher than that on non-event days. Instead, A_{Fuchs} varies
23 greatly among days in Beijing with a geometric standard deviation of 2.56, while it is relatively stable at other locations
24 such as Tecamac, Atlanta, and Boulder. Good correlation was found between A_{Fuchs} and L_{Γ} in Beijing ($R^2 = 0.88$). It
25 appears that the abundance of gaseous precursors such as sulfuric acid in Beijing is high enough to have nucleation,
26 however, it is A_{Fuchs} that determines the occurrence of NPF event in Beijing. 10 in 11 NPF events occurred when A_{Fuchs} is
27 smaller than $200 \mu\text{m}^2/\text{cm}^3$, and the NPF event was suppressed due to coagulation scavenging when A_{Fuchs} is larger than
28 $200 \mu\text{m}^2/\text{cm}^3$. Measured A_{Fuchs} is in good correlation with $\text{PM}_{2.5}$ mass concentration ($R^2 = 0.85$) since A_{Fuchs} in Beijing is
29 mainly determined by particles in the size range of 50 – 500 nm that also contribute to $\text{PM}_{2.5}$ mass concentration.



30 **1 Introduction**

31 New particle formation (NPF) is closely related to atmospheric environment and human life. It is a common atmospheric
32 phenomenon, which has been observed all over the world (Kulmala et al., 2004). High concentration of ultrafine particles
33 is formed intensively during a NPF event. It has been illustrated through both theoretical modelling and field observation
34 that these ultrafine particles can grow up to cloud condensation nuclei size (Kuang et al., 2009; Spracklen et al., 2008),
35 and thus affect climate (IPCC, 2013). The increased number concentration of ultrafine particles also raises concerns on
36 human health (HEI, 2013).

37 New particles are formed by nucleation from gaseous precursors such as sulfuric acid, ammonia, and organics. Newly
38 formed particles either grow up by condensation or are lost by coagulation with other particles (McMurry, 1983). Aerosol
39 Fuchs surface area, A_{Fuchs} , is a parameter that describes the coagulation scavenging effect quantitatively. In addition to
40 gaseous precursors participating in nucleation and subsequent condensational growth, it has been a consensus that the
41 occurrence of NPF event is also limited by A_{Fuchs} , because the survival possibility of nucleated particles is suppressed
42 when the coagulation scavenging effect is significant (Weber et al., 1997; Kerminen et al., 2001; Kuang et al., 2012).
43 Reported average A_{Fuchs} (or in the form of condensation sink) on NPF days was found to be lower than that on non-event
44 days at several locations (Dal Maso et al., 2005; Gong et al., 2010; Qi et al., 2015).

45 A dimensionless criterion, L_{Γ} , was proposed to characterize the ratio of particle scavenging loss rate over condensational
46 growth rate, and to predict the occurrence of NPF event in diverse atmospheric environment (Kuang et al., 2010). By
47 definition, L_{Γ} is determined by three factors, i.e., sulfuric acid concentration, the growth enhancement factor representing
48 contribution of other gaseous precursors in addition to sulfuric acid, Γ , and A_{Fuchs} . Sulfuric acid has a drastic diurnal
49 variation because of radiation, and the increase in sulfuric acid concentration after the sunrise can lead to nucleation.
50 A_{Fuchs} is often characterized in a narrow range at locations such as Tecamac, Atlanta, Boulder, and Hyytiälä (Kuang et al.,
51 2010), while sulfuric acid concentration among days may differ significantly at locations such as Atlanta and Hyytiälä
52 (Eisele et al., 2006; Petäjä et al., 2009) and it often governs nucleation and subsequent growth in the sulfur-rich
53 atmosphere such as in Atlanta (McMurry et al., 2005). The growth enhancement factor, Γ , may vary in a wide range at
54 locations such as Hyytiälä and may also fluctuate in a relative narrow range at other locations such as Tecamac and
55 Boulder.

56 Aerosol concentration in Beijing is usually much higher than that in clean environments. The annual average $\text{PM}_{2.5}$ mass
57 concentration in 2016 was $73 \mu\text{g}/\text{m}^3$ (reported by Beijing Municipal Environmental Protection Bureau), and the average
58 A_{Fuchs} measured in Beijing by this study was $381.5 \mu\text{m}^2/\text{cm}^3$, which is approximately a magnitude higher than those
59 measured in clean environments such as in Hyytiälä (Dal Maso et al., 2002). Different from comparatively slow



60 accumulation and depletion process of aerosol concentration in clean environments, A_{Fuchs} in Beijing may change rapidly
61 because of transport or accumulation of pollutants.

62 Sulfuric acid concentration is needed to estimate L_T , and direct measurement of particle size distribution down to ~ 1 nm
63 will help to better quantify NPF events. Although sulfuric acid has been measured around the world (Erupe et al., 2010),
64 and analysis based on sub-3 nm size distribution have been conducted sporadically since the development of diethylene
65 glycol scanning mobility particle spectrometer (DEG SMPS, Jiang et al., 2011a; Jiang et al., 2011b; Kuang et al., 2012)
66 and particle size magnifier (PSM, Vanhanen et al., 2011; Kulmala et al., 2013), there are limited data on atmospheric
67 sulfuric acid concentration and directly measured sub-3 particle size distributions in China. A campaign in Beijing during
68 2008 Olympic Games characterized atmospheric sulfuric acid concentration and its correlation with new particle
69 formation rate (Yue et al., 2010). The exponent in the correlation of formation rate, J_3 , with sulfuric acid was found to be
70 2.3, and the exponent for correlating derived $J_{1.5}$ with sulfuric acid was 2.7 (Wang et al., 2011), which were different from
71 the exponents between 1 and 2 often reported in other places around the world (Riipinen et al., 2007; Sihto et al., 2006;
72 Kuang et al., 2008). Sub-3 nm particle size distribution has not been reported previously in China except for 1-3 nm
73 particle number concentration in Shanghai in Winter 2013 inferred by a PSM (Xiao et al., 2015). Due to the limitation of
74 observation data, although good correlation was found between new particle formation rate and sulfuric acid concentration
75 in Beijing and the ratio of sulfuric acid concentration over A_{Fuchs} was found to positively correlate with number
76 concentration of 3-6 nm particles (Wang et al., 2011), the roles of sulfuric acid concentration and A_{Fuchs} in determining
77 the occurrence of NPF event have not been quantitatively illustrated.

78 In this study, we aimed to examine the roles of A_{Fuchs} and sulfuric acid in determining whether a NPF event will occur on
79 a particular day in Beijing. Data analysis was based on simultaneous measurement of particle size distributions down to
80 ~ 1 nm and sulfuric acid. Correlation between particle formation rate, $J_{1.5}$, and sulfuric acid concentration was examined.
81 L_T was used to predict the occurrence of NPF events, and relative daily variations of the three parameters determining L_T ,
82 i.e., sulfuric acid concentration, Γ , and A_{Fuchs} , were compared. A nominal value of A_{Fuchs} was suggested to predict the
83 occurrence NPF events in Beijing, and the relationship between $\text{PM}_{2.5}$ mass concentration and NPF events was also
84 examined.

85 2 Experiments

86 A field campaign studying NPF in Beijing was carried out from Mar. 7th to Apr. 7th, 2016. The campaign site was located
87 on the campus of Tsinghua University, and descriptions of this site can be found elsewhere (Cai & Jiang, 2017; He et al.,
88 2001). A home-made DEG SMPS was used to measure sub-5 nm particle size distribution and a particle size distribution
89 system (including a TSI aerodynamic particle sizer and two parallel SMPSSs, equipped with a TSI nanoDMA and a TSI



90 long DMA, respectively) was used to measure size distributions of particles from 3 nm to 10 μm (Liu et al., 2016). A
91 specially designed miniature cylindrical differential mobility analyser (mini- cyDMA) for effective classification of sub-
92 3 nm aerosol was equipped with the DEG SMPS (Cai et al., 2017). A cyclone was used at the sampling inlet to remove
93 particles larger than 10 μm . The sampled aerosol was subsequently dried by a silica-gel diffusion drier. The diameter
94 change due to drying was neglected when calculating A_{Fuchs} since the mean daytime relative humidity during the campaign
95 period was $\sim 25\%$. Diffusion losses, charging efficiency, penetration efficiencies through DMAs, detection efficiencies of
96 particle counters, and multi-charging effect were considered during data inversion. Particle density was assumed to be
97 1.6 g/cm^3 according to local observation results (Hu et al., 2012).

98 Sulfuric acid was measured by a modified high-resolution time-of-flight chemical ionization mass spectrometer (HR-
99 ToF-CIMS, Aerodyne Research Inc.). Instead of using radioactive ion source, a self-made corona discharge (CD) ion
100 source was utilized with the HR-TOF-CIMS. The CD ion source was design to be able to operate from a few Torr up to
101 near atmospheric pressure and has been successfully implemented in ambient amine (Zheng et al., 2015a) and
102 formaldehyde measurements (Ma et al., 2016). In this work, nitrate reagent ions were used to measure gaseous sulfuric
103 acid (Zheng et al., 2010). The detailed ion chemistry to generate nitrate ions and the sulfuric acid calibration procedures
104 have been detailed by Zheng et al. (2015b). Ambient sulfuric acid concentration in Beijing has been reported only once
105 in a field campaign conducted in 2008 (Zheng et al., 2011; Wang et al., 2011). Comparing to previous work, sulfuric acid
106 concentration reported in this study displayed similar diurnal variations, but with relatively lower daily maximum values.
107 This might due to the relatively weak solar radiation intensity encountered in this springtime observation than the previous
108 summertime campaign. To verify the precision of sulfuric acid measurement, the instrument was calibrated daily at night
109 and background checks were performed for ~ 3 minutes each hour during daytime.

110 A meteorological station (Davis 6250) was located ~ 10 m away from the sampling inlet at a comparatively open position,
111 measuring temperature, relative humidity, wind speed, wind direction, and precipitation. $\text{PM}_{2.5}$ mass concentration
112 measured in the nearest national monitoring station (Wanliu station, ~ 5 km away on the southwest of our campaign site)
113 was also used for analysis. Backward trajectories were obtained from online HYSPLIT server of national oceanic and
114 atmospheric administration (NOAA).

115 **3 Theory**

116 Nucleation is only the first step of new particle formation. Gaseous precursors form clusters by random collision and
117 bound together by Van der Waals force and/or chemical bond, and these clusters become particles if they are more likely
118 to grow by condensation rather than evaporate. However, particles formed by nucleation may be scavenged through
119 coagulation with larger particles before they grow large enough to be detected. Nucleation only refers to the process that



120 stable molecular clusters formed spontaneously from gaseous precursors, while new particle formation also requires
 121 subsequent condensational growth of freshly nucleated particles. That is, the occurrence of nucleation is mainly
 122 determined by gaseous precursors (e.g., sulfuric acid and organics) in atmospheric environment, while new particle
 123 formation is also influenced by the coagulation scavenging effect of pre-existing aerosols. Possibility exists that
 124 nucleation occurs while NPF events are not observed because of the short lifetime of nucleated particles due to the
 125 coagulation scavenging. In fact, nucleation can also be suppressed when aerosol concentration is high, since vapours and
 126 clusters may also be scavenged through diffusion onto aerosol surface.

127 Aerosol Fuchs surface area, A_{Fuchs} , is a representing parameter of coagulation scavenging based on kinetic theory, and it
 128 is corrected for particles whose size fall in the transition between free molecular regime and continuum regime (Davis et
 129 al., 1980; McMurry, 1983). The formula assuming unity coagulation efficiency (fraction of effective collisions) is shown
 130 in Eq. (1),

$$131 \quad A_{\text{Fuchs}} = \frac{4\pi}{3} \int_{d_{\min}}^{\infty} d_p^2 \cdot \left(\frac{Kn + Kn^2}{1 + 1.71Kn + 1.33Kn^2} \right) \cdot n \cdot dd_p, \quad (1)$$

132 where d_p is particle diameter, d_{\min} is the minimum particle diameter in theory and the measured minimum one in practice,
 133 Kn is Knudsen number and n is particle size distribution function, dN/dd_p . Condensation sink and coagulation sink can
 134 also describe how rapidly gaseous precursors and particles will be scavenged by pre-existing aerosol, respectively
 135 (Kerminen et al., 2001; Kulmala et al., 2001). Since condensation sink is proportional to A_{Fuchs} (McMurry et al., 2005)
 136 and coagulation sink can be approximately converted to condensation sink using a simple formula (Lehtinen et al., 2007),
 137 only A_{Fuchs} is used in this study to describe the coagulation scavenging effect and condensation sink reported in previous
 138 studies is referred in the form of A_{Fuchs} . The diffusion coefficient of sulfuric acid is assumed to be $0.117 \text{ cm}^2\text{s}^{-1}$ (Gong et
 139 al., 2010) when converting condensation sink into A_{Fuchs} .

140 A dimensionless criterion, L_T , have been proposed to predict the occurrence of NPF events (Kuang et al., 2010). It is
 141 defined as,

$$142 \quad L_T = \frac{\bar{c} \cdot A_{\text{Fuchs}}}{4\beta_{11}N_1} \cdot \frac{1}{\Gamma}, \quad (2)$$

143 where \bar{c} is the mean thermal speed of sulfuric acid which can be calculated from molecular kinetic theory; β_{11} is the
 144 coagulation coefficient between sulfuric acid monomers which can be calculated using Eq. 13.56 in Seinfeld & Pandis
 145 (2006); N_1 is the number concentration of sulfuric acid; and Γ is a growth enhancement factor and is defined as,

$$146 \quad \Gamma = \frac{2GR}{v_1N_m\bar{c}} \quad (3)$$

147 GR is the observed mean growth rate, v_1 is the corresponding volume of sulfuric acid monomer and it is estimated to be
 148 $1.7 \times 10^{-28} \text{ m}^3$ (approximately the volume of a hydrated sulfuric acid molecule, Kuang et al., 2010) in this study, and N_m is



149 the maximum number concentration of sulfuric acid during the whole period of a NPF event. Since other gaseous
 150 precursors in addition to sulfuric acid might also contribute to condensational growth of particles formed by nucleation
 151 (O'Dowd et al., 2002; Ristovski et al., 2010), while only concentration of sulfuric acid is used in Eq. (2), the ratio of
 152 measured growth rate over the growth rate assuming condensation of sulfuric acid (Weber et al., 1997), i.e., Γ , is used for
 153 correction. It should be clarified that L_T in Eq. (2) is defined similar to that in McMurry et al (2005) but slightly different
 154 from that in Kuang et al (2010), since L_T in this study are time-resolved values rather than event specific ones.
 155 Theoretically, Γ can also be time and size-resolved if using time and size-resolved GR and real-time concentration of
 156 sulfuric acid (Kuang et al., 2012), however, Γ during each NPF event is assumed to be constant in Eq. (3) because the
 157 validity of the improved model has not been tested. Note that the absolute concentration of sulfuric acid does not
 158 participate in calculation and thus has no influence on the results and conclusions reported in this study.

159 A new balance formula to estimate new particle formation rate was proposed recently (Cai & Jiang, 2017) and is given

160 below,

$$J_k = \frac{dN_{[d_k, d_u]}}{dt} + \sum_{d_g=d_k}^{d_u-1} \sum_{d_l=d_{\min}}^{+\infty} \beta_{(i,g)} N_{[d_l, d_{i+1}]} N_{[d_g, d_{g+1}]} - \frac{1}{2} \sum_{d_k=d_k}^{d_u-1} \sum_{\substack{d_i^3+d_{j+1}^3=d_k^3 \\ d_{i+1}^3+d_j^3=d_k^3 \\ d_i, d_j \geq d_{\min}}} \beta_{(i,j)} N_{[d_i, d_{i+1}]} N_{[d_j, d_{j+1}]} + n_u \cdot GR_u$$

161 , (4)

162 where J_k is the formation rate of particles at size d_k , $N_{[d_k, d_u]}$ is the total number concentration of particles from d_k to d_u
 163 (not included), d_u is the upper bound of the size range for calculation (25 nm in this study), d_{\min} is the size of minimum
 164 cluster in theory and the lower limit of measuring instrument in practice (1.3 nm in this study). The second and third
 165 terms in the right hand side of Eq. (4) are the coagulation sink term (*CoagSnk*) and the coagulation source term (*CoagSrc*),
 166 respectively. The difference between *CoagSnk* and *CoagSrc* is net *CoagSnk*, which represents the net rate of particles
 167 from d_k to d_u lost by coagulation scavenging. The last term is supposed to be negligible according to the determination
 168 criterions for d_u . dN/dt , which is the essential parameter representing the occurrence of NPF events, is actually the balance
 169 result of J_k , and net *CoagSnk*.

170 4 Results and Discussion

171 Total 26 days from Mar. 12th to Apr. 6th were classified by the occurrence of daytime NPF event. A typical NPF day is
 172 defined by intuitive features that distinct and persisting increasing of sub-3 nm particle concentration and subsequent
 173 growth of these nucleated particles. A day is classified as a non-event day if neither of these two features was observed.
 174 As shown in Fig. 1, 11 days are typical NPF days, 13 days are non-event days, and the rest two days were classified as
 175 undefined days. On these undefined days, i.e., Mar. 19th and Mar. 30th, the increase of sub-3 nm particle concentration
 176 and subsequent growth were both observed, however, sub-3 nm aerosol concentration was comparatively low and



177 evolution of particle size distributions was not continuous. NPF events mainly occurred when wind came from northwest
178 of Beijing, and the air mass mainly arrived at Beijing from southwest on non-event days (as summarized in Table 1). This
179 is because air mass coming from north usually experiences less influence from urban pollution, i.e., A_{Fuchs} is likely to be
180 lower than that on days dominated by southwest wind.

181 The dimensionless criterion, L_{Γ} , predicts NPF occurrence well in most days if unity was chosen as the threshold value.
182 L_{Γ} is the ratio of the rate at which particles are lost by coagulation over the growth rate. Larger L_{Γ} indicates higher
183 possibilities of nucleated particles to be scavenged by coagulation before they can continue to grow. Growth rates on non-
184 event days were assumed to 2.4 nm/h, which was the mean value of observed growth rates on NPF days (ranging from
185 1.2 nm/h to 3.3 nm/h). A threshold value of L_{Γ} can not be theoretically predicted but can be empirically estimated. 0.7
186 was suggested as the threshold value by Kuang et al. (2010), however, unity suggested by McMurry et al. (2005) seemed
187 to work better for NPF events observed in this campaign. Again, the nominal value of unity is only an empirical division
188 of NPF days and non-events days. In this campaign, median and mean value of L_{Γ} on NPF days were 0.55 and 0.71,
189 respectively, comparing to 3.05 and 3.45 on non-event days, respectively. However, some exceptions were also observed.
190 For instance, on the two undefined days, L_{Γ} were 1.40 and 0.64, respectively, and weak nucleation was observed.
191 Estimated L_{Γ} on Mar. 18th (an NPF event day) was 1.75, while a comparatively weak but still distinct NPF event was
192 observed. Despite these few exceptions, L_{Γ} works well in most cases in this campaign and were verified in other places
193 as well (Kuang et al., 2010). Following discussions will be focused on the contribution of different factors, i.e., sulfuric
194 acid concentration, Γ , and A_{Fuchs} .

195 **4.1 The Role of Gaseous Precursors**

196 Positive correlation was found between estimated new particle formation rate, $J_{1.5}$, and sulfuric acid concentration during
197 most NPF periods. On NPF days, the increase of sub-3 nm particle concentration was accompanied with the increase of
198 sulfuric acid concentration (as shown in Fig. 2). $J_{1.5}$ and sulfuric acid monomer concentration was only correlated during
199 NPF periods considering the possible sensitivity of the fitted parameters to the fitting time period (Kuang et al., 2008),
200 and the mean coefficient of determination during NPF periods in this campaign, R^2 , was 0.53. The exponents in the
201 correlation of the $J_{1.5}$ and sulfuric acid monomer concentration ranged from 1.5 to 4.0 in the 10 days with a mean value
202 of 2.4 (Mar. 29th is not included because of insignificant correlation), which is in consensus with reported mean exponent
203 of 2.3 using J_3 in Beijing (Wang et al., 2011). However, this result is quite different from those exponents no larger than
204 2 measured in North America and Europe (Kuang et al., 2008; Riipinen et al., 2007; Sihto et al., 2006), indicating
205 activation or kinetic nucleation alone can not explain the main nucleation mechanism on some days in this campaign.
206 Although correlation between sulfuric acid and particle formation was significant, sulfuric acid appeared not to be the
207 determining factor for whether a NPF event would occur, judging by the behaviour of sulfuric acid concentration. As



208 illustrated by time series of sulfuric acid concentration in Fig. 2, significant diurnal variation was observed every day.
209 However, the difference of daily maximum sulfuric acid concentration was small. The daily variations of sulfuric acid
210 concentration were significantly smaller than those of A_{Fuchs} . For instance, the geometrical standard deviation and relative
211 standard deviation of maximum sulfuric acid concentration on each day were 1.40 and 0.34, respectively, while those of
212 daily averaged A_{Fuchs} were 2.56 and 0.82, respectively. Sulfuric acid concentration during NPF periods was not
213 significantly higher than that between 8:00 - 16:00 on non-event days ($p=1$). In addition, comparatively high concentration
214 of sulfuric acid, e.g., on Apr. 4th - 6th, did not necessarily lead to NPF events.

215 The influence of growth enhancement factor, Γ , on the occurrence of NPF also needs to be addressed because sulfuric
216 acid alone may not explain the observed condensation growth. Estimated Γ values were normalized by dividing geometric
217 mean value during the campaign to compare with those in previous studies (Kuang et al., 2010); MILAGRO in Tecamac
218 (Iida et al., 2008); ANARChE (McMurry et al., 2005) in Atlanta; Boulder (Iida et al., 2006); QUEST II (Sihto et al.,
219 2006), QUEST IV (Riipinen, et al., 2007), and EUCCARI (Manninen et al., 2009) at the SMEAR II station in Hyytiälä.
220 It should be clarified that the relative value of Γ can improve the comparability by overcoming some uncertainties in
221 measuring sulfuric acid concentration by different studies. Fig. 4 indicates that Γ observed in this study distributes in a
222 relatively narrow range, similar to those observed in Tecamac, Atlanta, and Boulder, while different from the wide-
223 spreading characteristics observed in Hyytiälä. Geometric standard deviations of Γ were 1.31, 1.75, 2.23, 1.87, 1.62, 2.77,
224 and 2.87 in this campaign, MILAGRO, ANARChE, Boulder, QUEST II, QUEST IV, and EUCCARI, respectively. The
225 daily variations of Γ in this work were smaller than those observed in other places. They were also smaller than the daily
226 variations of A_{Fuchs} measured in this campaign. Considering the small daily variations of both sulfuric acid concentration
227 and Γ , it was reasonable to conclude that the abundance of sulfuric acid in Beijing during the campaign period was
228 sufficiently high for nucleation to occur but the occurrence of NPF events appeared to be governed by A_{Fuchs} .

229 **4.2 Relationship between A_{Fuchs} and NPF Event**

230 Relatively smaller A_{Fuchs} were found during most of the NPF days, while sulfuric acid concentrations on NPF days were
231 not significantly higher than that on non-event days. NPF events mainly occurred when A_{Fuchs} was smaller than 200
232 $\mu\text{m}^2/\text{cm}^3$, and non-event days mainly corresponded to real-time A_{Fuchs} larger than 200 $\mu\text{m}^2/\text{cm}^3$ and average A_{Fuchs} larger
233 than 350 $\mu\text{m}^2/\text{cm}^3$ (Fig. 5). The value of 200 $\mu\text{m}^2/\text{cm}^3$ appeared to be an empirical division between NPF days and non-
234 event days. If A_{Fuchs} was lower than this value, NPF event tended to occur, otherwise the occurrence of NPF event was
235 suppressed because of the predominant coagulation scavenging effect.

236 The variation of L_{Γ} in Beijing was governed by A_{Fuchs} . The measured L_{Γ} and A_{Fuchs} were in good correlation with a
237 coefficient of determination, R^2 , of 0.88, and the relative error of fitted L_{Γ} using A_{Fuchs} was 11.4% compared to the
238 measured ones (Fig. 6(a)). It should be clarified that GR on non-event days in this campaign were assumed to be the same



239 (2.4 nm/h, average of fitted values on NPF days), however, the correlation between L_T and A_{Fuchs} on NPF days alone
240 showed a R^2 of 0.89. A_{Fuchs} of $200 \mu\text{m}^2/\text{cm}^3$ corresponded to a L_T of approximately unity in this campaign. Since L_T has
241 been verified as a proper nucleation criterion in diverse atmospheric environment, it is reasonable to conclude that A_{Fuchs}
242 was the determining factor of the occurrence of NPF events in Beijing during the campaign period.

243 The A_{Fuchs} dominated characteristic of NPF events in Beijing showed a different pattern from those at other locations. L_T
244 and A_{Fuchs} in most other places do not correlate well (as shown in Fig. 6(b)) indicating that A_{Fuchs} alone could not predict
245 the occurrence of NPF events at these locations. Governing factors for the occurrence of NPF events at different locations
246 are illustrated in Fig. 10. At locations such as in Atlanta and Hyytiälä, A_{Fuchs} was observed to fluctuate within relatively
247 narrow ranges, while concentration of gaseous precursors participating in nucleation differed significantly. The variations
248 of L_T at these locations were mainly the consequence of relatively large variations in the concentrations of gaseous
249 precursors. However, the contribution of gaseous precursors to L_T was relatively stable in Beijing, while the variation of
250 L_T was mainly caused by varying A_{Fuchs} .

251 The predominant role of A_{Fuchs} in Beijing can also be explained by using the balance formula shown in Eq. (4). It is dN/dt
252 rather than formation rate, J , that directly reflects whether a NPF event has occurred or not, and dN/dt is the balance result
253 of formation rate and net $CoagSnk$ ($CoagSnk^- - CoagSrc$). Different from L_T which is the ratio of particle loss rate over
254 growth rate, the ratio of net $CoagSnk$ over J represents how many nucleated particles are lost to coagulation scavenging,
255 while the surviving particles are reflected as the increment of particle number concentration in nucleation mode.
256 Nucleation mode (1-25 nm) was used in this study to estimate dN/dt caused by nucleation because newly formed particles
257 seldom grew beyond 25 nm in the evaluated time period. Surviving possibilities of nucleated particles can also be inferred
258 using growth rate and A_{Fuchs} (Weber et al., 1997; Kerminen & Kulmala, 2002; Kuang et al., 2012), however, we consider
259 the ratio of net $CoagSnk$ over J to be more accurate because it is based on measured particle size distributions. Note that
260 theoretically the ratio of new $CoagSnk$ over J can be larger than unity, corresponding to a negative dN/dt . However, for
261 better description of the occurrence of NPF event rather than the whole process including termination, only NPF period
262 when dN/dt was positive is considered here. On average, 70.0% of particles formed by nucleation were lost due to
263 coagulation scavenging on NPF days (as shown in Fig. 8), indicating high coagulation loss in Beijing even on NPF days.
264 When A_{Fuchs} was much higher, most nucleated particles were lost to coagulation scavenging rather than growing to larger
265 sizes such that few NPF events were observed. Theoretically, NPF event can occur everyday in Beijing if one can simply
266 remove pre-existing aerosols while keeping other atmospheric compositions the same.

267 It should be clarified that although with much less possibility, NPF events may also occur when A_{Fuchs} was larger than
268 $200 \mu\text{m}^2/\text{cm}^3$ in Beijing. In this campaign, a distinct NPF event was observed with a comparatively high A_{Fuchs} (on Mar.
269 18th) of $329 \mu\text{m}^2/\text{cm}^3$, which was significantly higher than the suggested threshold value of $200 \mu\text{m}^2/\text{cm}^3$. As indicated by



270 the content of Table 1, this exception was caused by the failure of L_T rather than A_{Fuchs} alone. The comparatively low
271 number concentration of sub-3 nm particles together with the moderate particle formation rate indicated that the NPF
272 event was suppressed. In addition, NPF events previously reported in Beijing occurred when A_{Fuchs} was relatively high
273 (Wu et al., 2007; Wang et al., 2013; Wang et al., 2017) with a maximum A_{Fuchs} value of $\sim 555 \mu\text{m}^2/\text{cm}^3$ (Kulmala et al.,
274 2016). The A_{Fuchs} reported in these studies might be overestimated because daily average rather than average over NPF
275 event period only was used. For instance, A_{Fuchs} in Beijing during non-event period can be significantly higher and it may
276 change rapidly because of transport or subsequent growth of nucleated particles. Nevertheless, A_{Fuchs} can be considered
277 as the major determining factor of the occurrence of NPF events in Beijing, while admitting that exceptions can
278 occasionally occur at a medium L_T larger than unity, corresponding to A_{Fuchs} larger than $200 \mu\text{m}^2/\text{cm}^3$.

279 4.3 A case Study of 3 Days

280 Three continuous days including two NPF days and one non-event day are shown in Fig. 9 to further illustrate the roles
281 of A_{Fuchs} and sulfuric acid (together with other gaseous precursors) in affecting the occurrence of NPF events in Beijing.
282 On Apr. 2nd, A_{Fuchs} maintained at a relative low level and NPF event occurred after sunrise together with the increase in
283 sulfuric acid concentration, and ended in the afternoon when sulfuric acid concentration decreased to a low level. The
284 whole NPF event began at approximately 7:30 and ended at approximately 14:30, which was also the typical time period
285 for other NPF days. However, on Apr. 3rd, wind direction changed from northwest into southwest at noon, sulfuric acid
286 concentration decreased, and A_{Fuchs} increased rapidly because of transport of particles from south, causing the increase in
287 L_T . The ongoing NPF event was interrupted and no newly nucleated particles was observed even though sulfuric acid
288 concentration increased later. On Apr. 4th, A_{Fuchs} was at a high level, causing L_T to be always larger than unity. Sulfuric
289 acid concentration on Apr. 4th was higher than those on Apr. 2nd and 3rd, however, no NPF event was observed. Therefore,
290 even though the abundance of gaseous precursors in Beijing often seemed to be high enough for nucleation to happen,
291 whether or not an NPF event to occur was mainly governed by A_{Fuchs} .

292 4.4 Predicting NPF Days Using $\text{PM}_{2.5}$ Mass Concentration

293 A rough but simple parameter, i.e., $\text{PM}_{2.5}$ mass concentration, can also be applied to predict whether an NPF event can
294 happen in Beijing. Theoretically, the exponent in the relationship between A_{Fuchs} and particle diameter is between 1 and
295 2 depending on particle size (as shown in Eq. (1)), while particle mass is proportional to the 3rd power of particle diameter.
296 Hence the correlation between A_{Fuchs} and mass concentration can be determined by particle size distributions.
297 Accumulation mode particles ranged from 50 nm to 500 nm was the major contribution to A_{Fuchs} in Beijing, and
298 normalized size distribution of accumulation mode particles were relative stable at different A_{Fuchs} levels (as shown in
299 Fig. 11). On NPF days when A_{Fuchs} were relatively low, nucleation mode particles formed by nucleation and subsequent



300 growth also contributed to A_{Fuchs} , however, A_{Fuchs} was still governed by accumulation mode particles. Thus, A_{Fuchs} should
301 show better correlation with particle mass concentration rather than number concentration. Figure 10 indicates that there
302 is a good correlation between A_{Fuchs} and $\text{PM}_{2.5}$ mass concentration in Beijing with a R^2 of 0.85, although the correlation
303 at low A_{Fuchs} level is not as good as that at high A_{Fuchs} level because of influence of particles formed by nucleation.
304 Measured $\text{PM}_{2.5}$ mass concentration in the 26 days ranged from 3 to $420 \mu\text{g}/\text{m}^3$, which was wide enough to represent both
305 relative clean days and severe polluted days in Beijing. $\text{PM}_{2.5}$ mass concentrations during NPF periods were mostly
306 smaller than $30 \mu\text{g}/\text{m}^3$ except for the case of Mar. 18th and it was higher than $30 \mu\text{g}/\text{m}^3$ between 8:00 and 16:00 on non-
307 event days. Note that the threshold of $30 \mu\text{g}/\text{m}^3$ may not be valid for the whole year since it was based on field
308 measurement in March and early April and the concentration of gaseous precursors perhaps varied with season because
309 of different radiation intensity and emissions.

310 The criterion using $\text{PM}_{2.5}$ mass concentration was applied to predict NPF events measured at the same site in Beijing in
311 April and May, 2014. Among 38 days in that campaign, 11 typical NPF events were identified. Average $\text{PM}_{2.5}$ mass
312 concentration during NPF period was lower than $30 \mu\text{g}/\text{m}^3$ in 9 NPF events, while that in the rest two days was 49.8 and
313 $40.5 \mu\text{g}/\text{m}^3$, respectively. In another campaign in Beijing during January 2016, 12 in 14 NPF events were observed to
314 occur when daily mean $\text{PM}_{2.5}$ mass concentration was less than $30 \mu\text{g}/\text{m}^3$ (the maximum value on NPF days was 43
315 $\mu\text{g}/\text{m}^3$), and $\text{PM}_{2.5}$ mass concentration on 16 non-event days were all larger than $40 \mu\text{g}/\text{m}^3$ (Jayaratne et al., 2017).

316 Conclusions

317 Factors governing the occurrence of NPF events in Beijing were examined using data from a field campaign during Mar.
318 12th to Apr. 6th, 2016. In these 26 days, 11 typical NPF event days were observed. The rest were 2 undefined days and 13
319 non-event days. New particle formation rate, $J_{1.5}$, was in positive correlation with sulfuric acid concentration with a fitted
320 mean exponent of 2.4, however, sulfuric acid concentration on NPF days was not significantly higher than that on non-
321 event days. A dimensionless criterion proposed by Kuang et al. (2010), L_{Γ} , was found to be applicable to predict NPF
322 event in most days. Theoretically, L_{Γ} was determined by sulfuric acid concentration, the enhancement factor, Γ , and Fuchs
323 surface area, A_{Fuchs} , together. However, A_{Fuchs} alone was found to be in good correlation with L_{Γ} ($R^2 = 0.88$) in Beijing.
324 Different from NPF events observed at other locations such as Hyytiälä, the variations of daily maximum sulfuric acid
325 concentration and the enhancement factor in Beijing were in a narrow range with geometric standard deviations of 1.40
326 and 1.31, respectively, while A_{Fuchs} varied significantly among days with a geometric standard deviation of 2.56. It was
327 inferred that the concentrations of gaseous precursors such as sulfuric acid in Beijing were high enough to cause
328 nucleation, while it was A_{Fuchs} that ultimately determined whether a NPF event would occur or not in Beijing. In this work,
329 we proposed that an A_{Fuchs} of $200 \mu\text{m}^2/\text{cm}^3$ can be used as the empirical threshold value, below which NPF events were



330 highly likely to occur in Beijing. However, NPF events would be suppressed when A_{Fuchs} was higher than this threshold
331 value. The A_{Fuchs} dominated characteristic of NPF events in Beijing was different from those at other locations such as
332 Atlanta, Boulder, and Hyytiälä. Since A_{Fuchs} in Beijing was mainly governed by accumulation mode particles (50 to 500
333 nm) and in this size range the normalized $dA_{\text{Fuchs}}/d\log d_p$ was relatively stable at different A_{Fuchs} levels, measured A_{Fuchs}
334 was in good correlation with $\text{PM}_{2.5}$ mass concentration ($R^2 = 0.85$). Accordingly, $\text{PM}_{2.5}$ mass concentration may also
335 serve as a rough and simple parameter to predict the occurrence of NPF events in Beijing. An empirical threshold value
336 of $30 \mu\text{g}/\text{m}^3$ was proposed based on data from this field campaign and was found to work well for other field campaigns
337 in Beijing as well.

338 Acknowledgement

339 Financial supports from the National Science Foundation of China (21422703, 41227805, 21521064, 21377059 &
340 41575122) and the National Key R&D Program of China (2014BAC22B00, 2016YFC0200102 & 2016YFC0202402)
341 are acknowledged.

342 References

- 343 Cai, R., Chen, D.-R., Hao, J., & Jiang, J.: A Miniature Cylindrical Differential Mobility Analyzer for sub-3 nm Particle
344 Sizing. *Journal of Aerosol Science*, 106, 111-119, doi:10.1016/j.jaerosci.2017.01.004, 2017.
- 345 Cai, R., & Jiang, J.: A new balance formula to estimate particle formation rate: reevaluating effect of coagulation
346 scavenging. *Atmospheric Chemistry and Physics Discussion*, doi:10.5194/acp-2017-199, in review, 2017.
- 347 Dal Maso, M., Kulmala, M., Lehtinen, K.E., Mäkelä, J.M., Aalto, J., & O'Dowd, C.D.: Condensation and coagulation
348 sinks and formation of nucleation mode particles in coastal and boreal forest boundary layers. *Journal of*
349 *Geophysical Research*, 107, doi:10.1029/2001jd001053, 2002.
- 350 Dal Maso, M., Kulmala, M., Riipinen, I., Wagner, R., Hussein, T., Aalto, P., & Lehtinen, K.E.: Formation and growth of
351 fresh atmospheric aerosols: eight years of aerosol size distribution data from SMEAR II, Hyytiälä, Finland.
352 *Boreal Environment Research*, 10, 323-336, 2005.
- 353 Davis, E.J., P., R., & K., R.A.: A Review of Theory and Experiments on Diffusion from Submicroscopic Particles.
354 *Chemical Engineering Communications*, 5, 251-268, 1980.
- 355 Eisele, F.L., Lovejoy, E.R., Kosciuch, E., Moore, K.F., Mauldin, R.L., Smith, J.N., McMurry, P.H., & Iida, K.: Negative
356 atmospheric ions and their potential role in ion-induced nucleation. *Journal of Geophysical Research*, 111,
357 doi:10.1029/2005jd006568, 2006.
- 358 Erupe, M.E., Benson, D.R., Li, J., Young, L.-H., Verheggen, B., Al-Refai, M., Tahboub, O., Cunningham, V., Frimpong,
359 F., Viggiano, A.A., & Lee, S.-H.: Correlation of aerosol nucleation rate with sulfuric acid and ammonia in Kent,
360 Ohio: An atmospheric observation. *Journal of Geophysical Research*, 115, doi:10.1029/2010jd013942, 2010.
- 361 Gong, Y., Hu, M., Cheng, Y., Su, H., Yue, D., Liu, F., Wiedensohler, A., Wang, Z., Kalesse, H., & Liu, S.: Competition
362 of coagulation sink and source rate: New particle formation in the Pearl River Delta of China. *Atmospheric*
363 *Environment*, 44, 3278-3285, doi:10.1016/j.atmosenv.2010.05.049, 2010.
- 364 He, K., Yang, F., Ma, Y., Zhang, Q., Yao, X., Chan, C.K., Cadel, S., Chan, T., & Mulawa, P.: The characteristics of $\text{PM}_{2.5}$
365 in Beijing, China. *Atmospheric Environment*, 35, 4959-4970, 2001.



- 366 HEI Review Panel on Ultrafine Particles: Understanding the Health Effects of Ambient Ultrafine Particles. HEI
367 Perspectives 3. Health Effects Institute, Boston, MA, 2013.
- 368 Hu, M., Peng, J., Sun, K., Yue, D., Guo, S., Wiedensohler, A., & Wu, Z.: Estimation of size-resolved ambient particle
369 density based on the measurement of aerosol number, mass, and chemical size distributions in the winter in
370 Beijing. *Environmental science & technology*, 46, 9941-9947, doi:10.1021/es204073t, 2012.
- 371 Iida, K., Stolzenburg, M., McMurry, P., Dunn, M.J., Smith, J.N., Eisele, F., & Keady, P.: Contribution of ion-induced
372 nucleation to new particle formation: Methodology and its application to atmospheric observations in Boulder,
373 Colorado. *Journal of Geophysical Research: Atmospheres*, 111, doi:10.1029/2006jd007167, 2006.
- 374 Iida, K., Stolzenburg, M.R., McMurry, P.H., & Smith, J.N.: Estimating nanoparticle growth rates from size-dependent
375 charged fractions: Analysis of new particle formation events in Mexico City. *Journal of Geophysical Research:*
376 *Atmospheres*, 113, doi:10.1029/2007jd009260, 2008.
- 377 IPCC.: *Climate Change 2013: IPCC Fifth Assessment Report (AR5)*. Cambridge University Press, 2013.
- 378 Jayaratne, R., Pushpawela, B., He, C., Gao, J., Hui, L., Morawska, L.: Observations of Particles at their Formation Sizes
379 in Beijing, China. *Atmospheric Chemistry and Physics Discussions*, doi:10.5194/acp-2017-156, in review, 2017.
- 380 Jiang, J., Chen, M., Kuang, C., Attoui, M., & McMurry, P.H.: Electrical Mobility Spectrometer Using a Diethylene Glycol
381 Condensation Particle Counter for Measurement of Aerosol Size Distributions Down to 1 nm. *Aerosol Science*
382 *and Technology*, 45, 510-521, doi:10.1080/02786826.2010.547538, 2011.
- 383 Jiang, J., Zhao, J., Chen, M., Eisele, F.L., Scheckman, J., Williams, B.J., Kuang, C., & McMurry, P.H.: First
384 Measurements of Neutral Atmospheric Cluster and 1–2 nm Particle Number Size Distributions During
385 Nucleation Events. *Aerosol Science and Technology*, 45, ii-v, doi:10.1080/02786826.2010.546817, 2011.
- 386 Kerminen, V.M., & Kulmala, M.: Analytical formulae connecting the "real" and the "apparent" nucleation rate and the
387 nuclei number concentration for atmospheric nucleation events. *Journal of Aerosol Science*, 33, 609-622, 2002.
- 388 Kerminen, V.-M., Pirjola, L., & Kulmala, M.: How significantly does coagulation scavenging limit atmospheric particle
389 production? *Journal of Geophysical Research: Atmospheres*, 106, 24119-24125, doi:10.1029/2001jd000322,
390 2001.
- 391 Kuang, C., Chen, M., Zhao, J., Smith, J., McMurry, P.H., & Wang, J.: Size and time-resolved growth rate measurements
392 of 1 to 5 nm freshly formed atmospheric nuclei. *Atmospheric Chemistry and Physics*, 12, 3573-3589,
393 doi:10.5194/acp-12-3573-2012, 2012.
- 394 Kuang, C., McMurry, P. H., & McCormick, A. V.: Determination of cloud condensation nuclei production from measured
395 new particle formation events, *Geophysical Research Letters*, 36, doi:10.1029/2009gl037584, 2009.
- 396 Kuang, C., McMurry, P.H., McCormick, A.V., & Eisele, F.L.: Dependence of nucleation rates on sulfuric acid vapor
397 concentration in diverse atmospheric locations. *Journal of Geophysical Research*, 113,
398 doi:10.1029/2007jd009253, 2008.
- 399 Kuang, C., Riipinen, I., Sihto, S.L., Kulmala, M., McCormick, A.V., & McMurry, P.H.: An improved criterion for new
400 particle formation in diverse atmospheric environments. *Atmospheric Chemistry and Physics*, 10, 8469-8480,
401 doi:10.5194/acp-10-8469-2010, 2010.
- 402 Kulmala, M., Dal Maso, M., Mäkelä, J. M., Pirjola, L., Väkevä, M., Aalto, P., Miikkulainen, P., Hämeri, K., and O'Dowd,
403 C. D.: On the formation, growth and composition of nucleation mode particles, *Tellus*, 53, 479-490, 2001.
- 404 Kulmala, M., Kontkanen, J., Junninen, H., Lehtipalo, K., Manninen, H.E., Nieminen, T., Petäjä, T., Sipilä, M.,
405 Schobesberger, S., Rantala, P., Franchin, A., Jokinen, T., Jarvinen, E., Äijälä, M., Kangasluoma, J., Hakala, J.,
406 Aalto, P.P., Paasonen, P., Mikkilä, J., Vanhanen, J., Aalto, J., Hakola, H., Makkonen, U., Ruuskanen, T.,
407 Mauldin, R.L., 3rd, Duplissy, J., Vehkamäki, H., Bäck, J., Kortelainen, A., Riipinen, I., Kurtén, T., Johnston,
408 M.V., Smith, J.N., Ehn, M., Mentel, T.F., Lehtinen, K.E., Laaksonen, A., Kerminen, V.-M., & Worsnop, D.R.:
409 Direct observations of atmospheric aerosol nucleation. *Science*, 339, 943-946, doi:10.1126/science.1227385,
410 2013.



- 411 Kulmala, M., Petäjä, T., Kerminen, V.-M., Kujansuu, J., Ruuskanen, T., Ding, A., Nie, W., Hu, M., Wang, Z., Wu, Z.,
412 Wang, L., & Worsnop, D.R.: On secondary new particle formation in China. *Frontiers of Environmental Science*
413 & *Engineering*, 10, doi:10.1007/s11783-016-0850-1, 2016.
- 414 Kulmala, M., Vehkamäki, H., Petäjä, T., Dal Maso, M., Lauri, A., Kerminen, V.M., Birmili, W., & McMurry, P.H.:
415 Formation and growth rates of ultrafine atmospheric particles: a review of observations. *Journal of Aerosol*
416 *Science*, 35, 143-176, doi:10.1016/j.jaerosci.2003.10.003, 2004.
- 417 Lehtinen, K.E.J., Dal Maso, M., Kulmala, M., & Kerminen, V.-M.: Estimating nucleation rates from apparent particle
418 formation rates and vice versa: Revised formulation of the Kerminen–Kulmala equation. *Journal of Aerosol*
419 *Science*, 38, 988-994, doi:10.1016/j.jaerosci.2007.06.009, 2007.
- 420 Liu, J., Jiang, J., Zhang, Q., Deng, J., & Hao, J.: A spectrometer for measuring particle size distributions in the range of
421 3 nm to 10 µm. *Frontiers of Environmental Science & Engineering*, 10, 63-72, doi:10.1007/s11783-014-0754-
422 x, 2016.
- 423 Ma, Y., Diao, Y., Zhang, B., Wang, W., Ren, X., Yang, D., Wang, M., Shi, X., and Zheng, J.: Detection of formaldehyde
424 emissions from an industrial zone in the Yangtze River Delta region of China using a proton transfer reaction
425 ion-drift chemical ionization mass spectrometer. *Atmospheric Measurement Techniques*, 9, 6101-6116, 2016.
- 426 Manninen, E.H., Petäjä, T., Asmi, E., Riipinen, I., Nieminen, T., Mikkilä, J., Hörrak, U., Mirme, A., Mirme, S., Laakso,
427 L., Kerminen, V.-M., & Kulmala, M.: Long-term field measurements of charged and neutral clusters using
428 Neutral cluster and Air Ion Spectrometer (NAIS). *Boreal Environment Research*, 2009, 591-605, 2009.
- 429 McMurry, P.H. New particle formation in the presence of an aerosol: rates, time scales, and sub-0.01 µm size distributions
430 *Journal of Colloid and Interface Science*, 95, 72-80, 1983.
- 431 McMurry, P.H., Fink, M., Sakurai, H., Stolzenburg, M.R., Mauldin, R.L., Smith, J., Eisele, F., Moore, K., Sjostedt, S.,
432 Tanner, D., Huey, L.G., Nowak, J.B., Edgerton, E., & Voisin, D.: A criterion for new particle formation in the
433 sulfur-rich Atlanta atmosphere. *Journal of Geophysical Research*, 110, doi:10.1029/2005jd005901, 2005.
- 434 O'Dowd, C.D., Aalto, P., Hmeri, K., Kulmala, M., & Hoffmann, T.: Aerosol formation: atmospheric particles from
435 organic vapours. *Nature*, 416, 497-498, doi:10.1038/416497a, 2002.
- 436 Petäjä, T., Mauldin, R.L., Kosciuch, E., McGrath, J., Nieminen, T., Paasonen, P., Boy, M., Adamov, A., Kotiaho, T., &
437 Kulmala, M.: Sulfuric acid and OH concentrations in a boreal forest site. *Journal of Aerosol Science*, 9, 7435-
438 7448, 2009.
- 439 Qi, X.M., Ding, A.J., Nie, W., Petäjä, T., Kerminen, V.-M., Herrmann, E., Xie, Y.N., Zheng, L.F., Manninen, H., Aalto,
440 P., Sun, J.N., Xu, Z.N., Chi, X.G., Huang, X., Boy, M., Virkkula, A., Yang, X.-Q., Fu, C.B., & Kulmala, M.:
441 Aerosol size distribution and new particle formation in the western Yangtze River Delta of China: 2 years of
442 measurements at the SORPES station. *Atmospheric Chemistry and Physics*, 15, 12445-12464, doi:10.5194/acp-
443 15-12445-2015, 2015.
- 444 Riipinen, I., Sihto, S.-L., Kulmala, M., Arnold, F., Dal Maso, M., Birmili, W., Saarnio, K., Teinilä, K., Kerminen, V.-M.,
445 Laaksonen, A., & Lehtinen, K.E.J.: Connections between atmospheric sulphuric acid and new particle formation
446 during QUEST III-IV campaigns in Heidelberg and Hyytiälä. *Atmospheric Chemistry and Physics*, 7, 1899-
447 1914, doi:10.5194/acp-7-1899-2007, 2007.
- 448 Ristovski, Z.D., Suni, T., Kulmala, M., Boy, M., Meyer, N., K., Duplissy, J., Turnipseed, A., Morawska, L., &
449 Baltensperger, U.: The role of sulphates and organic vapours in growth of newly formed particles in a eucalypt
450 forest. *Atmospheric Chemistry and Physics*, 10, 2919-2926, 2010.
- 451 Seinfeld, J.H., & Pandis, S.N.: *Atmospheric Chemistry and Physics* (2nd ed.). John Wiley & Sons, Inc., New Jersey,
452 2006.
- 453 Sihto, S.L., Kulmala, M., Kerminen, V.M., Dal Maso, M., Petäjä, T., Riipinen, I., Korhonen, H., Arnold, F., Janson, R.,
454 Boy, M., Laaksonen, A., & Lehtinen, K.E.: Atmospheric sulphuric acid and aerosol formation: implications from
455 atmospheric measurements for nucleation and early growth mechanisms. *Atmospheric Chemistry and Physics*,
456 6, 4079-4091, 2006.



- 457 Spracklen, D.V., Carslaw, K.S., Kulmala, M., Kerminen, V.-M., Sihto, S.-L., Riipinen, I., Merikanto, J., Mann, G.W.,
 458 Chipperfield, M.P., Wiedensohler, A., Birmili, W., & Lihavainen, H.: Contribution of particle formation to
 459 global cloud condensation nuclei concentrations. *Geophysical Research Letters*, 35, doi:10.1029/2007gl033038,
 460 2008.
- 461 Vanhanen, J., Mikkilä, J., Lehtipalo, K., Sipilä, M., Manninen, H.E., Siivola, E., Petäjä, T., & Kulmala, M.: Particle Size
 462 Magnifier for Nano-CN Detection. *Aerosol Science and Technology*, 45, 533-542,
 463 doi:10.1080/02786826.2010.547889, 2011.
- 464 Wang, Z., Wu, Z., Yue, D., Shang, D., Guo, S., Sun, J., Ding, A., Wang, L., Jiang, J., Guo, H., Gao, J., Cheung, H.C.,
 465 Morawska, L., Keywood, M., & Hu, M.: New particle formation in China: Current knowledge and further
 466 directions. *The Science of the total environment*, 577, 258-266, doi:10.1016/j.scitotenv.2016.10.177, 2017.
- 467 Wang, Z.B., Hu, M., Sun, J.Y., Wu, Z.J., Yue, D.L., Shen, X.J., Zhang, Y.M., Pei, X.Y., Cheng, Y.F., & Wiedensohler,
 468 A.: Characteristics of regional new particle formation in urban and regional background environments in the
 469 North China Plain. *Atmospheric Chemistry and Physics*, 13, 12495-12506, doi:10.5194/acp-13-12495-2013,
 470 2013.
- 471 Wang, Z.B., Hu, M., Yue, D.L., Zheng, J., Zhang, R.Y., Wiedensohler, A., Wu, Z.J., Nieminen, T., & Boy, M.: Evaluation
 472 on the role of sulfuric acid in the mechanisms of new particle formation for Beijing case. *Atmospheric Chemistry
 473 and Physics*, 11, 12663-12671, doi:10.5194/acp-11-12663-2011, 2011.
- 474 Weber, R.J., Marti, J.J., McMurry, P.H., Eisele, F.L., Tanner, D.J., & Jefferson, A.: Measurements of new particle
 475 formation and ultrafine particle growth rates at a clean continental site. *Journal of Geophysical Research:
 476 Atmospheres*, 102, 4375-4385, doi:10.1029/96jd03656, 1997.
- 477 Wu, Z., Hu, M., Liu, S., Wehner, B., Bauer, S., Maßling, A., Wiedensohler, A., Petäjä, T., Dal Maso, M., & Kulmala,
 478 M.: New particle formation in Beijing, China: Statistical analysis of a 1-year data set. *Journal of Geophysical
 479 Research*, 112, 2007.
- 480 Xiao, S., Wang, M.Y., Yao, L., Kulmala, M., Zhou, B., Yang, X., Chen, J.M., Wang, D.F., Fu, Q.Y., Worsnop, D.R., &
 481 Wang, L.: Strong atmospheric new particle formation in winter in urban Shanghai, China. *Atmospheric
 482 Chemistry and Physics*, 15, 1769-1781, 10, doi:1029/2006jd007406, 2015.
- 483 Yue, D. L., Hu, M., Zhang, R. Y., Wang, Z. B., Zheng, J., Wu, Z. J., Wiedensohler, A., He, L. Y., Huang, X. F., and Zhu,
 484 T.: The roles of sulfuric acid in new particle formation and growth in the mega-city of Beijing. *Atmospheric
 485 Chemistry and Physics*, 10, 4953-4960, doi:10.5194/acp-10-4953-2010, 2010.
- 486 Zheng, J., Khalizov, A., Wang, L., and Zhang, R.: Atmospheric pressure-ion drift chemical ionization mass spectrometry
 487 for detection of trace gas species. *Analytical Chemistry*, 82, doi:10.1016/j.atmosenv.2014.05.024, 7302-7308,
 488 2010.
- 489 Zheng, J., Hu, M., Zhang, R., Yue, D., Wang, Z., Guo, S., Li, X., Bohn, B., Shao, M., He, L., Huang, X., Wiedensohler,
 490 A., and Zhu, T.: Measurements of gaseous H₂SO₄ by AP-ID-CIMS during CAREBeijing 2008 Campaign.
 491 *Atmospheric Chemistry and Physics*, 11, 7755-7765, doi:10.5194/acp-11-7755-2011, 2011.
- 492 Zheng, J., Ma, Y., Chen, M., Zhang, Q., Wang, L., Khalizov, A. F., Yao, L., Wang, Z., Wang, X., and Chen, L.:
 493 Measurement of atmospheric amines and ammonia using the high resolution time-of-flight chemical ionization
 494 mass spectrometry. *Atmospheric Environment*, 102, 249-259, doi:10.1016/j.atmosenv.2014.12.002, 2015a.
- 495 Zheng, J., Yang, D., Ma, Y., Chen, M., Cheng, J., Li, S., and Wang, M.: Development of a new corona discharge based
 496 ion source for high resolution time-of-flight chemical ionization mass spectrometer to measure gaseous H₂SO₄
 497 and aerosol sulfate. *Atmospheric Environment*, 119, 167-173, doi:10.1016/j.atmosenv.2015.08.028, 2015b.

498

499 **Table 1: Summary of parameterized descriptions for each campaign day.**

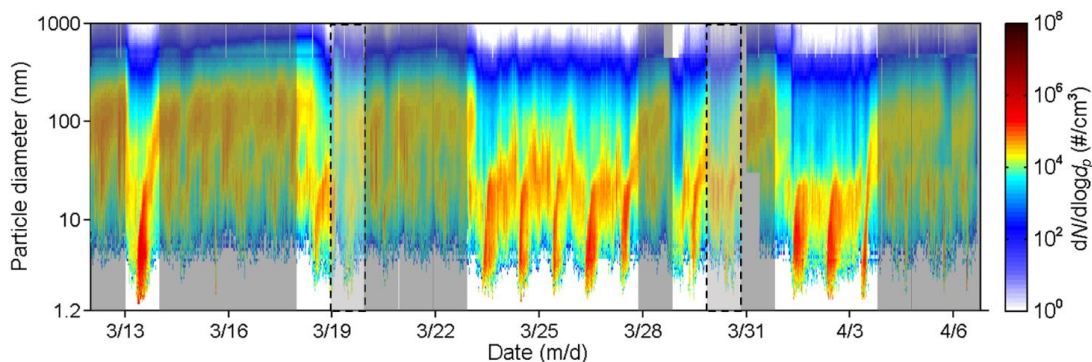
Date (mm/dd)	Classification	Max $J_{1.5}$ ($\text{cm}^{-3} \text{s}^{-1}$)	N_{1-3}^*	A_{Fuchs}^*	L_T^*	Wind direction*
-----------------	----------------	---	-------------	----------------------	---------	--------------------



		(#/cm ³)		(μm ² /cm ³)		
03/12	Non-event	–	0	919.5	3.63	SW
03/13	NPF	156.0	26347.5	119.7	0.71	NW
03/14	Non-event	–	0	632.7	3.05	NW
03/15	Non-event	–	0	733.9	3.73	SW
03/16	Non-event	–	0	796.2	4.15	WSW
03/17	Non-event	–	0	1140.1	9.04	WSW
03/18	NPF	33.8	741.2	329.0	1.75	WNW
03/19	Undefined	Weak**	1643.67	240.8	1.40	SE
03/20	Non-event	–	137.9	348.8	1.74	NNW
03/21	Non-event	–	0	512.0	2.76	SSW
03/22	Non-event	–	0	457.6	2.58	E
03/23	NPF	30.1	3846.3	76.1	0.57	NNW
03/24	NPF	46.8	5576.7	145.2	0.76	NNW
03/25	NPF	57.0	4637.7	126.7	0.52	NNE
03/26	NPF	41.5	9640.9	100.4	0.71	N
03/27	NPF	31.2	2806.2	90.6	0.44	NW
03/28	Non-event	–	0	508.1	2.86	W
03/29	NPF	32.3	2449.8	121.0	0.69	NW
03/30	Undefined	17.7	2885.7	88.8	0.64	NW
03/31	Non-event	–	0	767.0	4.21	SW
04/01	NPF	50.9	5477	51.7	0.22	WNW
04/02	NPF	46.9	10002	63.1	0.31	NW
04/03	NPF	21.6	10962.9	105.7	0.24	NW
04/04	Non-event	–	442	398.2	3.09	SW
04/05	Non-event	–	185	391.2	2.33	NW
04/06	Non-event	–	0	365.5	1.71	SW

500 *: Indicated by 12-hour backward trajectory (starting at noon, 500 m in altitude). **: Difficult to estimate.

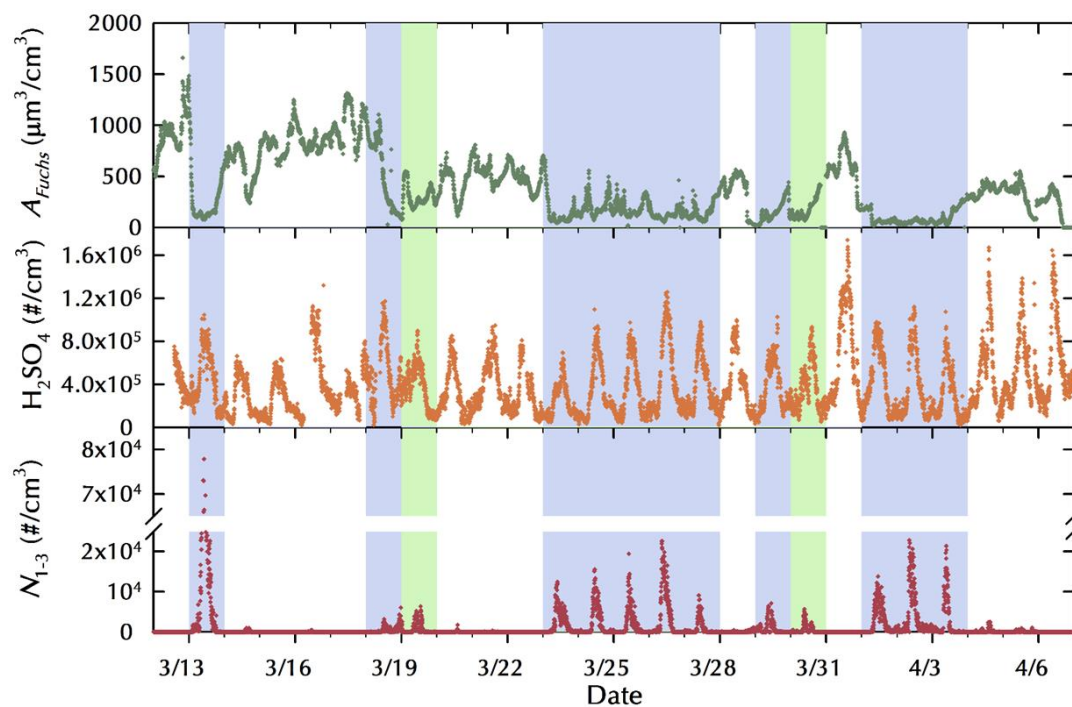
501



502

503 **Figure 1** Contour of measured particle size distribution during Mar. 12th to Apr. 6th. Identified thirteen non-event days are

504 shadowed by grey colour. Two undefined days are shadowed by lighter grey boxes with dashed lines as the edges.

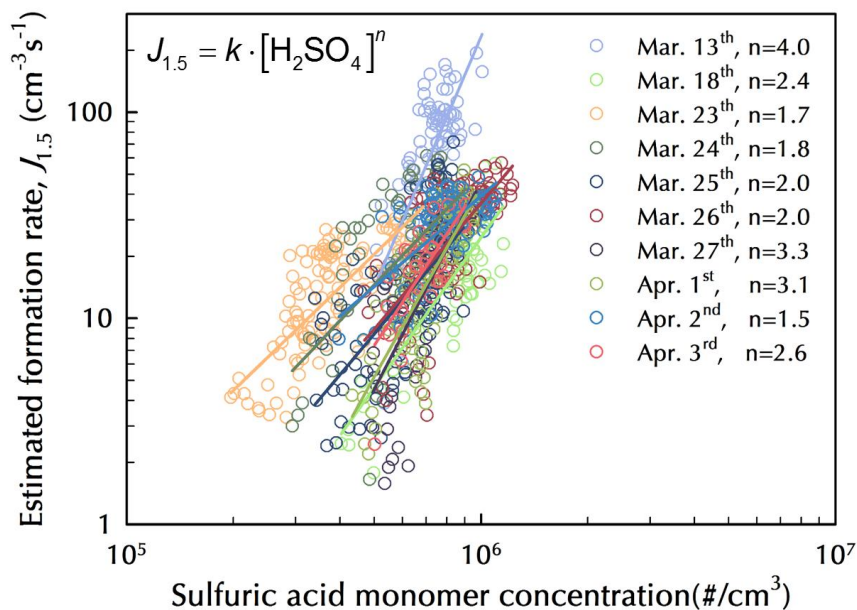


505

506 **Figure 2:** Time series for Fuchs surface area (A_{Fuchs}), sulfuric acid concentration, and number concentration of 1-3 nm particles.

507 Typical NPF days and undefined days are shadowed by light blue and light green background, respectively.

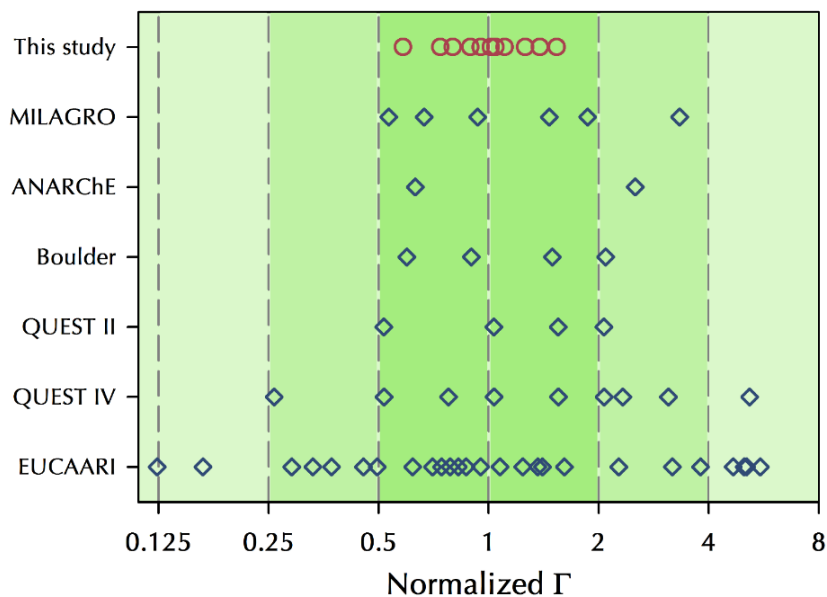
508



509

510 **Figure 3: Correlations between estimated new particle formation rate, $J_{1.5}$, and number concentration of sulfuric acid monomer**
511 **during NPF period on each NPF day. Regression line of $J_{1.5}$ versus sulfuric acid monomer concentration is exponentially fitted,**
512 **where n is the exponent. Data on Mar. 29th is not included because the correlation between $J_{1.5}$ and sulfuric acid monomer**
513 **concentration was not significant ($p = 0.34$).**

514

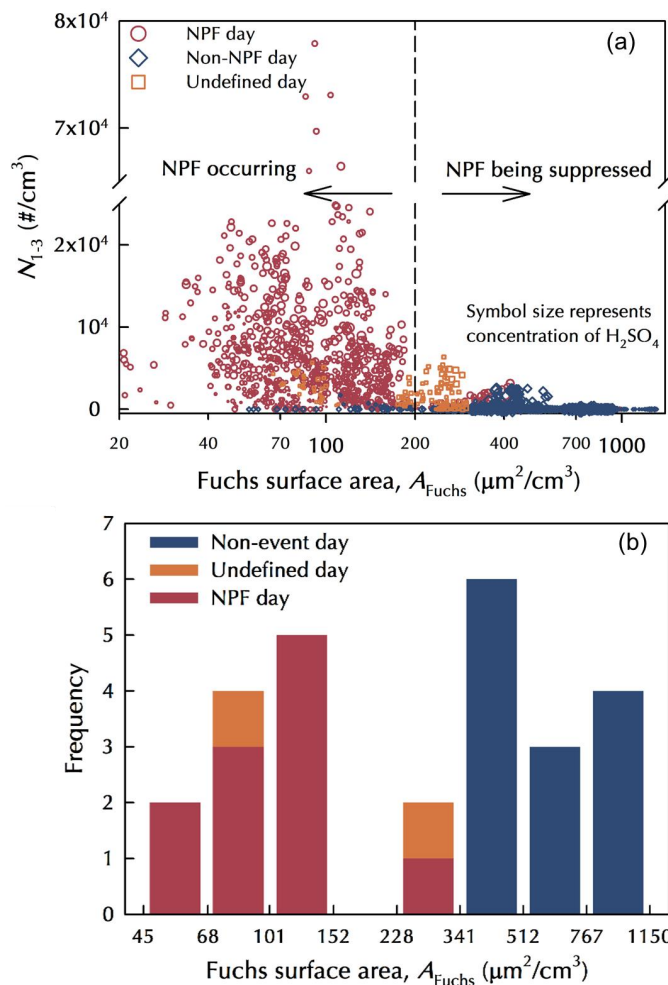


515

516 **Figure 4: Normalized growth enhancement factor, Γ , in this campaign and previous ones. Γ is normalized by the geometric**

517 **mean value in each campaign.**

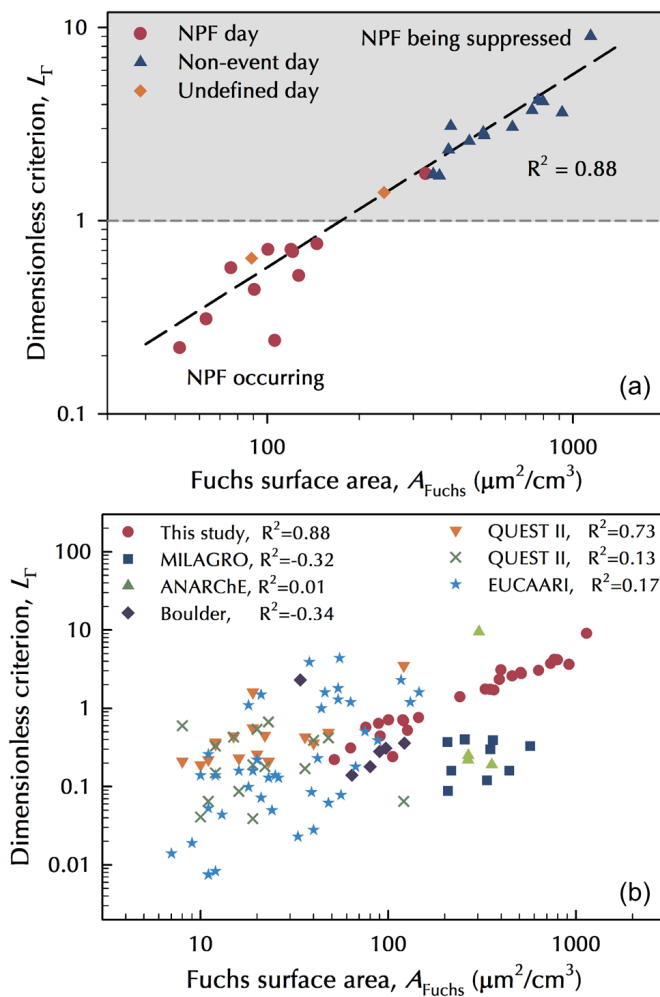
518



519

520 **Figure 5:** (a) Relationship between Fuchs surface area and number concentration of 1-3 nm particles, N_{1-3} . Relative
 521 concentration of measured sulfuric acid is represented by symbol size, i.e., the higher the relative concentration, the bigger the
 522 symbol size. Data points are 5-minute-resolved. (b) Histogram of frequency of observed NPF days, undefined days and non-
 523 event days sorting by daily average Fuchs surface area. On typical NPF days and undefined days, A_{Fuchs} was averaged during
 524 NPF period. On non-event days, it was averaged between 8:00 and 16:00. Values of A_{Fuchs} were binned in logarithmic scale
 525 ranging from 45 to 1150.

526



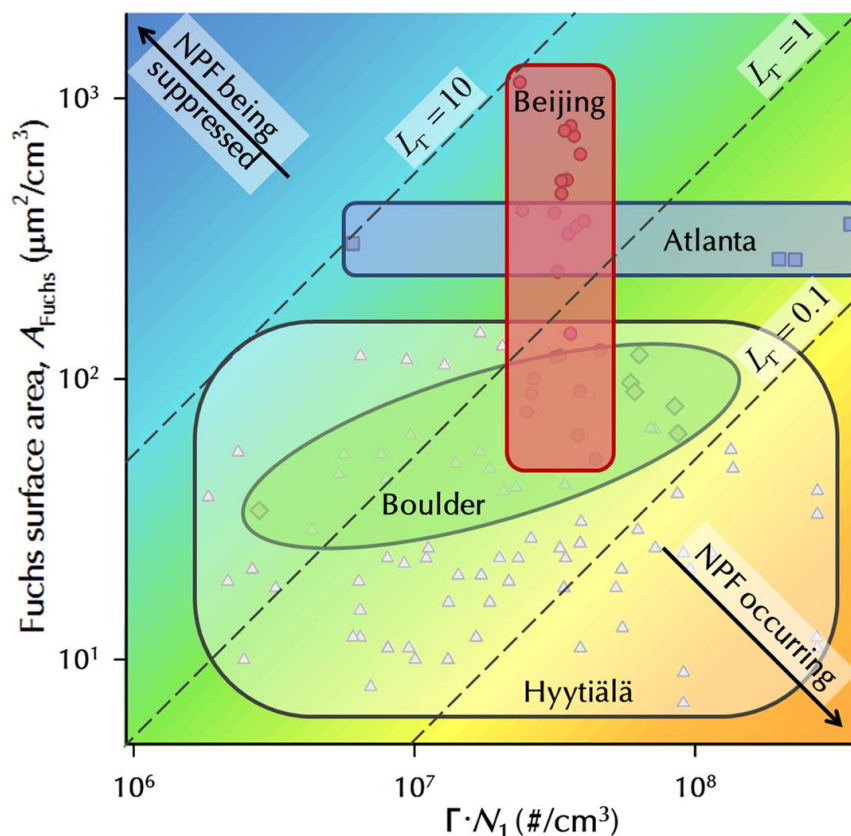
527

528 **Figure 6: (a) Correlation between L_T and A_{Fuchs} (data from Table 1) in this campaign. NPF days, non-event days, and**

529 **undefined days are shown by different symbols, while regression is base on all observation days. (b) Correlation between L_T**

530 **and A_{Fuchs} in previous studies and this campaign.**

531



532

533 **Figure 7: Schematic of governing factors for L_r at different locations. Concentration of growth relevant gaseous precursors**

534 **is represented by $\Gamma \cdot N_1$, where Γ is the growth enhancement factor and N_1 is number concentration of sulfuric acid.**

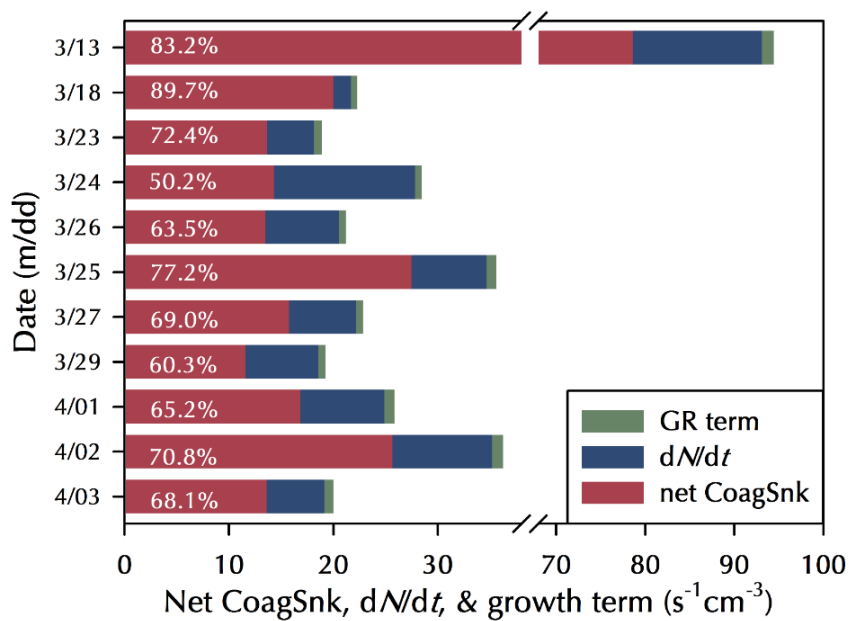
535 **Background colour represents the value of L_r . Observed data at each locations are shown in different symbols (circle:**

536 **Beijing; square: Atlanta; diamond: Boulder; triangle: Hyytiälä), while the ellipse and the boxes are artificially drawn to**

537 **illustrate the ranges of data points at different locations. Tecamac was not included because of lacking data on non-event**

538 **days. Both axes are in log scale.**

539



540

541

Figure 8: Average contribution of net CoagSnk, dN/dt , and condensational growth term (GR term) to the estimated new particle

542

formation rate, $J_{1.5}$, on identified typical NPF days. The percentage presented in each column is the relative ratio of net CoagSnk

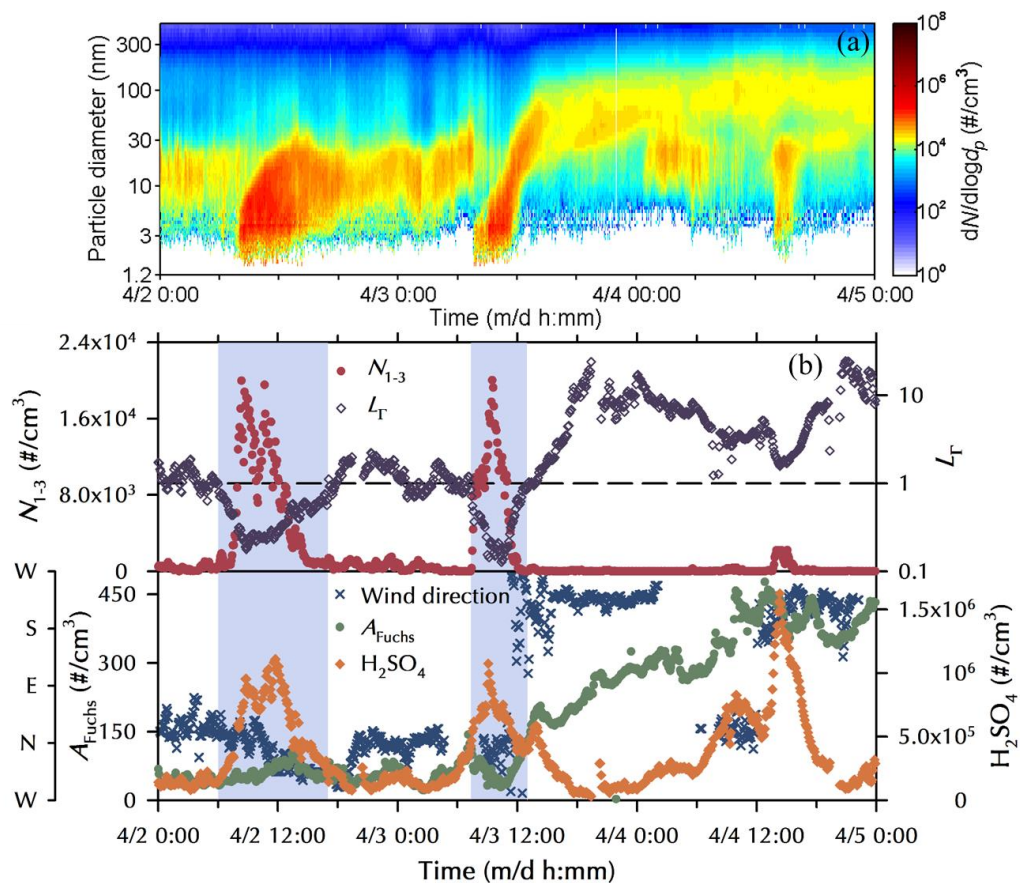
543

compared to $J_{1.5}$ in that NPF day. Note that only the time period when dN/dt is positive during a NPF event was taken in to

544

account when calculating average contribution.

545



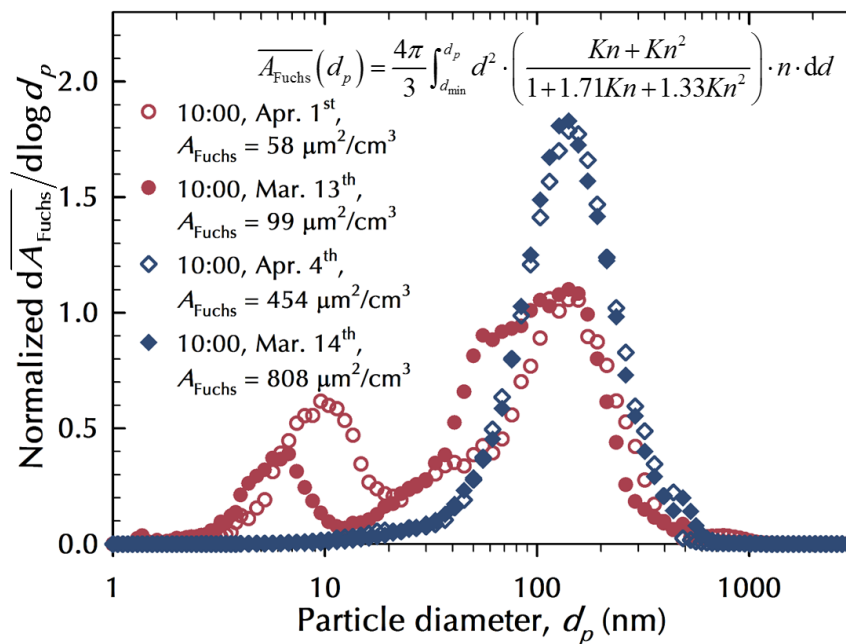
546

547 **Figure 9:** (a) Contour of measured particle size distribution on Apr. 2nd, 3rd, and 4th. (b) Representative parameters on these

548 three NPF days. Time period when L_T was smaller than 1.0 is shadowed by light blue background. Wind direction data is

549 obtained from local meteorological station and it is not shown when the wind speed was close to zero.

550



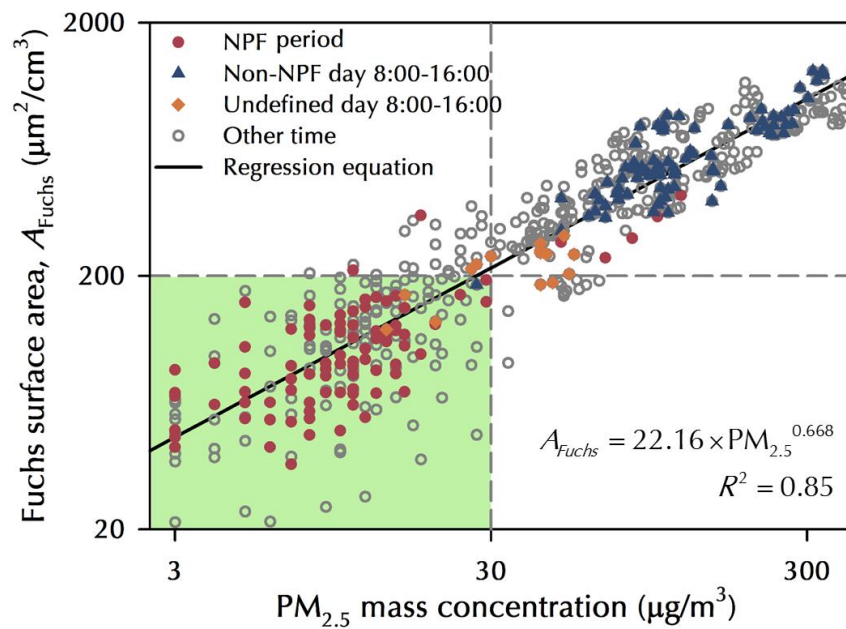
551

552 **Figure 10:** Normalized distribution of cumulative Fuchs surface area, $\overline{A_{\text{Fuchs}}}$, as a function of particle diameter, d_p , on two

553 NPF days (red circle) and two non-event days (blue diamond). $\overline{A_{\text{Fuchs}}}$ is equal to A_{Fuchs} when d_p is approaching positive infinity.

554 $\overline{dA_{\text{Fuchs}}/d\log d_p}$ is normalized by dividing A_{Fuchs} .

555



556

557 **Figure 11: Relationship between hourly averaged A_{Fuchs} and $PM_{2.5}$ mass concentration in Beijing. Data during the time period**

558 **when A_{Fuchs} changed rapidly is not included to avoid potential influence caused by the distance between Wanliu station and our**

559 **campaign site. NPF period, daytime (8:00-16:00) on non-event days and undefined days, and other time is represented by**

560 **different symbols, while the regression of A_{Fuchs} versus $PM_{2.5}$ mass concentration is based on all these data. The proposed**

561 **criterion for NPF event, i.e., A_{Fuchs} smaller than $200 \mu\text{m}^2/\text{cm}^3$ which approximately corresponds to $PM_{2.5}$ mass concentration**

562 **smaller than $30 \mu\text{g}/\text{cm}^3$, is shadowed by light green.**

563